DE GRUYTER Nanotechnology Reviews 2023; 12: 20220521

Review Article

Liang Sun*[#], Xiongshuai Ji[#], Yong Zhou, Hang Li, Wenyan Zhai*, Biqiang Chen, Hui Dong, Yanmin Liu, and Tengwei Wang

An overview of hydrogen production from Al-based materials

https://doi.org/10.1515/ntrev-2022-0521
received December 31, 2021; accepted February 9, 2023

Abstract: A profound overview of the recent development for on-time, on-demand hydrogen production from light metal-based hydrolysis is presented. Hydrogen energy is one of the clean and renewable energy sources which has been recognized as an alternative to fossil fuels. In addition, aluminum is the most suitable light activity metal for hydrolysis materials attributed to its safety, environmental friendliness, high-energy density, inexpensive, and low density with high strength ratio. In general, dense oxide films formed act as a barrier on aluminum surfaces. Accordingly, effective removal of the oxide film is a key measure in solving the Al–water reaction. In this review, recent advances in addressing the main drawbacks including high-purity aluminum with acid–alkali solutions, nano-powders of aluminum or composite with acid–base solutions, ball-milled nano-powders, alloying blocks, and gas atomization powders are summarized. The characteristics of these three technologies and the current research progress are summarized in depth. Moreover, it is essential to promote low-cost aluminum-based materials based on effective hydrogen production efficiency and explore ways for practical large-scale applications.

Keywords: hydrogen energy, Al-based alloys, hydrolysis reaction, activation metals, ball milling

1 Introduction

Energy is considered a “strategic commodity,” while the volume of global energy trade has developed substantially over the past 30 years. For global countries, energy security is the cornerstone of national security and a primary consideration in energy trade strategies and policies [1,2]. Currently, more than 80% of human energy consumption is accounted for by fossil fuels (coal, oil, and natural gas). Nevertheless, renewable energy stands in contrast to traditional biomass, which is being used far more quickly than they are being replenished. Derse *et al.* [3] noted that “Hydrogen network management is one of the focal issues for a cleaner and sustainable world. The developed model is compatible with the real world issues by incorporating safety conditions. The sensitivity analysis indicates that distances are effective on the total cost.” An urgent demand for developing clean and renewable green energy sources has been evoked [4]. On the one hand, the main cause of global warming was fossil fuels with an increase in the atmospheric greenhouse gas levels [5,6]. On the other hand, uniformly distributed fossil fuels which are controlled by certain countries globally raise conflicts regarding the security of supply and distribution in developing countries. Ultimately, finite sources of energy will be eventually depleted, and global competition and price increase of these resources

---

[#] These authors contributed equally to this work and should be considered first co-authors.

---

* **Corresponding author: Liang Sun**, Key Laboratory of Materials Processing Engineering, College of Materials Science and Engineering, Xi’an Shiyou University, Xi’an, 029, China, e-mail: lsun@xsyu.edu.cn
* **Corresponding author: Wenyan Zhai**, Key Laboratory of Materials Processing Engineering, College of Materials Science and Engineering, Xi’an Shiyou University, Xi’an, 029, China, e-mail: 180606@xsyu.edu.cn
Xiongshuai Ji: Key Laboratory of Materials Processing Engineering, College of Materials Science and Engineering, Xi’an Shiyou University, Xi’an, 029, China, e-mail: 19212050519@stumail.xsyu.edu.cn
Yong Zhou: Key Laboratory of Materials Processing Engineering, College of Materials Science and Engineering, Xi’an Shiyou University, Xi’an, 029, China, e-mail: yzhou@xsyu.edu.cn
Hang Li: Shaanxi Environmental Protection Group Ecological Construction Management Co., Ltd. Xi’an, 029, China
Biqiang Chen: Xi’an Thermal Power Research Institute Co., Ltd., Xi’an 710054, China
Hui Dong: Key Laboratory of Materials Processing Engineering, College of Materials Science and Engineering, Xi’an Shiyou University, Xi’an, 029, China, e-mail: donghui@xsyu.edu.cn
Yanmin Liu: Key Laboratory of Materials Processing Engineering, College of Materials Science and Engineering, Xi’an Shiyou University, Xi’an, 029, China, e-mail: ymliu@xsyu.edu.cn
Tengwei Wang: Key Laboratory of Materials Processing Engineering, College of Materials Science and Engineering, Xi’an Shiyou University, Xi’an, 029, China, e-mail: wtw_xsyu@163.com

cannot be ruled out in the future [7]. In response to increasing energy demand and low carbon needs, green and renewable energy has become a political and economic focal point finally [8]. For instance, Europe has committed to reducing greenhouse gas emissions by 80–95% below the 1990 levels by 2050 [9]. Of course, widening the utilization of solar, wind, hydro, and tidal natural energy can significantly reduce greenhouse gas emissions; however, they cannot be regulated because of intermittent sources [10,11]. The grid requires a certain percentage of stationary energy as a base; thus, storing clean energy is critical during this transformation. In order to phase out fossil fuels and limit climate change, hydrogen energy is considered the most promising option [9,12]. Hydrogen energy is a clean and renewable energy source and several advantages are as follows:

1) Abundant reserves. Mainly in the form of hydrocarbons and water, and hydrogen is one of the most readily available elements on earth [13].
2) Excellent energy density (122 kJ/g). Approximately 2.75 times more than that of hydrocarbon fuels [14].
3) Non-toxic and non-polluting. Water is the only combustion product [15,16].
4) Wide range of applications. High heat capacity can be benefited from hydrogen combustion to produce mechanical work in a heat engine, or as an energy material for fuel cells to generate electricity directly [17–19].

Hydrogen is a key chain between hydrogen-consuming industries and several essential sectors such as the electricity grid, gas grid, transportation, residential, agriculture, and energy storage [20]. Therefore, hydrogen energy is the most promising clean energy source at this stage [21,22]. Currently, fossil fuel hydrogen production methods have occupied the largest proportion of industrial hydrogen production (to date, the total volume of hydrogen consumption was 48% from natural gas, 30% from heavy oils and naphtha, and 18% from coal) [23–26]. Clearly, it is not in line with the strategic requirements of sustainable development in the world [27].

Thus, alternative methods of hydrogen production are urgently needed [24,28–32]. As shown in Figure 1, the production, application, and storage of hydrogen play a key role, yet it is always a challenge. As the density of hydrogen is only 7.14% of air density [33] and the ignition energy is only 0.02 mJ [14,34,35], special attention should be paid to safety issues during transportation. Metal hydrolysis behaves as a feature of convenient storage and transportation in hydrogen technology [36], which can provide on-time and on-demand hydrogen production. On the one hand, the replacement of large volumes, large weights, high-pressure resistant, or adiabatic hydrogen storage bottles can effectively avoid the safety problems during high-pressure gaseous hydrogen storage applications and low-temperature liquid hydrogen storage. On the other hand, infrastructure construction is suitable for gas applications in various special scenarios such as disaster area rescue, emergency power supply, field detection, single-armed combat, *etc.*

The theoretical hydrogen release content of aluminum (Al) is 11.1%, which is higher than that of Na (4.34%), Mg (8.3%), and Fe (3.57%) [37]. The production of hydrogen by hydrolysis reaction of hydrides (Mg and MgH_2, $NaBH_4$, $LiAlH_4$, Al, *etc.*) recently attracted increased attention because of its safety and its amenability to mild reaction conditions. For example, in recent years, more and more attention has been paid to hydrogen generation by hydrolysis of metals, metal hydrides, or formic acid for their high theoretical hydrogen yield [38–41]. Generally, the energy efficiencies of the MgH_2, H–Mg_3La, and H–La_2Mg_{17} hydrolysis cycles were 45.3, 40.1, and 41.1%, respectively, for half of the energy released by the exothermic reaction from this cycle was collected for recycling. However, the maximum energy efficiency (49.91%) indicates that the reaction of MgH_2 with $NaBO_2$ to form $NaBH_4$ during ball milling is feasible [42,43]. Additionally, aluminum is the most abundant metal in the earth's crust with a low density of 2,700 kg/m^3. Likewise, it is of low cost and has high gravimetric and volumetric energy density and high energy efficiency (31.1 MJ/kg and 83.8 MJ/L) [44]. The Al–water reactions are as follows:

$$2Al + 6H_2O \rightarrow 2Al(OH)_3 + 3H_2, \tag{1}$$

$$2Al + 4H_2O \rightarrow 2AlO(OH) + 3H_2. \tag{2}$$

According to reactions (1) and (2), 1 mol Al can produce 1.5 mol H_2. Under theoretically standard conditions, 1,245 mL of hydrogen can be generated from 1 g of aluminum. The end-products of Al–water reaction ($Al(OH)_3$, AlO(OH)) are non-toxic, non-polluting, and easy to collect and store. Other advantages include wide applications in flame retardants [45,46], adsorbents [47], *etc.* Therefore, the Al–water reaction can provide safe, environmentally friendly, and portable hydrogen energy. Furthermore, regeneration is a potential method for reducing the cost, and a one-step approach for hydrogen production, storage, and transportation is a new method *via* Li(Na)BH_4 regeneration using Mg-based alloys and as the new topics for hydrogen-energy process chain and hydrogen economics [48–50].

This overview briefly introduced various hydrogen production technologies for aluminum-based materials, compared the development trends of each technology, and provided an outlook on the future advanced methods for aluminum-based materials. Theoretically, since the Gibbs free energy $\Delta G < 0$ for the Al–water reaction, it means the reaction direction can conduct spontaneously with water.

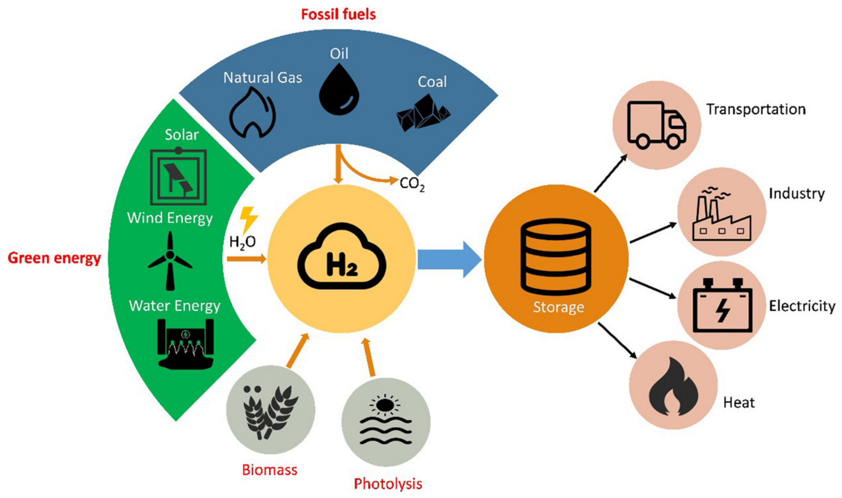

Figure 1: Importance of hydrogen in integrating different energy sectors.

However, a dense alumina film is formed on the Al-based material surface for its activity, which prevents the Al–water reaction from proceeding [51,52]. Hence, eliminating the oxide layer is a key point to the problem of Al–water reaction.

2 Reaction with acid or alkali solution

Al_2O_3 is the main component of the dense film on the surface of aluminum which can react with both acid and alkali solutions at room temperature. The reaction mechanism among HCl is displayed as follows:

$$Al_2O_3 + 6HCl \rightarrow 2AlCl_3 + 3H_2O, \tag{3}$$

$$2Al + 6HCl \rightarrow 2AlCl_3 + 3H_2. \tag{4}$$

The acid solution reacts with Al_2O_3 first to destroy the outer oxide layer and then contacts the inner pure aluminum matrix, as evident from reactions (3) and (4). This reaction can evoke hydrogen generation directly. However, the H^+ concentration decreases and the pH increases during the reaction. The hydrogen generation rate is bound to decrease whenever the acid supplementation is stopped. However, aluminum reacts differently with alkali solutions, and the surface aluminum passivation layer dissolved more easily than in acidic solutions. The reaction equations are given as follows [53–55]:

$$Al_2O_3 + 2NaOH \rightarrow 2NaAlO_2 + H_2O, \tag{5}$$

$$2Al + 6H_2O + 2N_aOH \rightarrow 2NaAl(OH)_4 + 3H_2, \tag{6}$$

$$NaAl(OH)_4 \rightarrow NaOH + Al(OH)_3. \tag{7}$$

First, the Al_2O_3 layer begins to dissolve in NaOH solution at the outer oxide layer. In other words, aluminum starts to lose its protective film and NaOH in the solution is consumed by the oxide layer and $NaAl(OH)_4$ is produced, which in turn decomposes into NaOH again. Finally, aluminum directly reacts with water. During this whole process, NaOH does not participate in the Al–water reaction and only plays a role as a catalyst. Hiraki *et al.* [56] described the reaction of aluminum with sodium hydroxide solution which is shown in Figure 2. The schematic diagram of the experimental apparatus is shown in Figure 2(a), while the hydrogen generation and rate were detected with a flow meter. As shown in Figure 2(b), the content of H_2 increases with time and the hydrogen generation rate starts to decrease after a certain time. When H_2 is produced, the solution temperature increases rapidly. In addition, the pH of the solution decreases in the first period and then increases. The consumption of NaOH is mainly due to the formation of $Al(OH)_4^-$ first, and then $Al(OH)_4^-$ decomposes to $Al(OH)_3$ and OH^-. This reaction continues and moves in circles. Additionally, NaOH promotes the Al–water reaction more efficiently than KOH and $Ca(OH)_2$ [57], while the reaction rate can be further increased by the temperature and the surface area of aluminum increased. In addition, the reaction rate is also strongly influenced by the concentration of the base solution. The consistency of CO_2 in the air decreases the concentration gradient of free hydroxides in aqueous solutions and the reaction rate [58,59].

Although this kind of reaction provides a compact source of hydrogen, it is not suitable for practical use because highly concentrated acid and alkali solutions can corrode the equipment, and strict control of the pH of the solution is required to achieve good hydrolysis results.

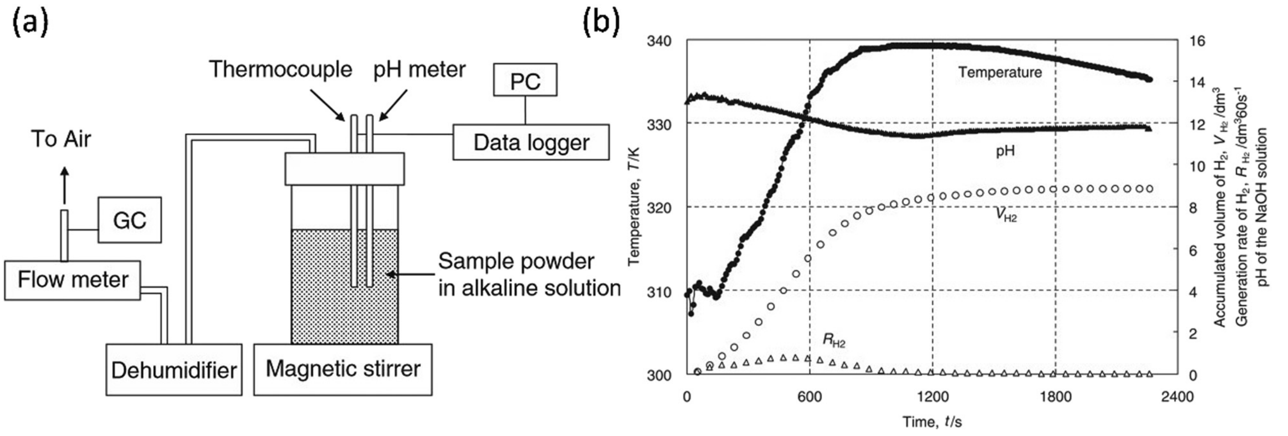

Figure 2: (a) Schematic diagram of the experimental apparatus (b) Time evolution of the temperature and pH of the NaOH aqueous solution, the accumulated volume and the generation rate of hydrogen [56].

3 Hydrolysis reactions of ball-milled aluminum matrix composites

A powerful means of activating aluminum is mechanical ball milling [60] which crushes the powder into particles by strongly impacting, grinding, and stirring the aluminum powder through mechanical alloying and milling [61,62]. In milling, large particles of metal are ground into small particles, and ball milling builds on this by converting small particles into nano-powder and forming new compounds between different metals; therefore, ball milling is a combination of mechanical alloying and milling. Generally, powders are susceptible to agglomeration during ball milling, which can deeply affect the hydrolysis reaction. Therefore, mixing aluminum with grinding aids (such as salts, metal oxides, or metal hydrides) for ball milling can effectively improve the hydrolytic activity of aluminum. During the ball milling process, the physical interaction occurs between the grinding aid and pores, cracks, and even fractures in the microstructure of the aluminum-based material, which not only deeply expands the specific surface area but also the distortion of the lattice structure and leads to elevated energy in the imperfections or defects of the metal matrix.

In this process, many active reaction sites are formed to promote the Al–water reaction [63,64]. The details of different grinding aids are discussed below.

3.1 Salt additives

Generally, NaCl is a common grinding aid in aluminum ball milling due to its low cost, safety, non-toxicity, good solubility, and environmentally friendly. NaCl addition in ball milling directly continuously chops or destroys the aluminum oxide layer of the aluminum powder and prevents the agglomeration of the powder. After activation of aluminum by mechanical treatment, NaCl particles embedded on the aluminum surface and a large number of pits on the aluminum surface emerged after dissolving in water, which increases the contact area of the Al–water reaction and promotes the reaction rate. Yolcular and Karaoglu [65] analyzed the relationship between the NaCl content and ball milling time for the aluminum powder during hydrogen production. It can be seen that without NaCl, as the ball milling time increases, the aluminum powder grows into spherical particles of 1–2 mm diameter due to agglomeration. If the NaCl content is increased from 5 to 20%, the diameter of the composite powder further decreased and the hydrogen generation rate reached 1,300 mL/(g min), as shown in Figure 3. The mixture with the addition of NaCl has a laminar structure and can exhibit better hydrolytic properties.

Irankhah *et al.* [66] explored the promotion of Al–water reaction by NaCl, KCl, and $BaCl_2$. In comparison with NaCl, KCl and $BaCl_2$ could cover the surface of Al effectively. As a result, $BaCl_2$ could significantly reduce the induction time of the reaction, while the alloy powders of hydrogen yield with $BaCl_2$ adjunction was considerably lower than that of NaCl and KCl. The hydrogen generation curve with different salt additives is shown in Figure 4. Chai *et al.* [61] investigated the effect of $CoCl_2$ and $NiCl_2$ on the Al–water reaction and found that the highest hydrogen yield was reached when the $CoCl_2$ concentration was increased from 0.5 to 1 M. Nevertheless, the hydrogen yield diminished significantly when the $CoCl_2$ concentration was further raised to 2 M. The effect of $CoCl_2$ and $NiCl_2$ concentrations on the hydrogen yield also showed similar trends. The reason was the formation of Co/Al and Ni/Al galvanic cells, which cause Co or Ni to aggregate

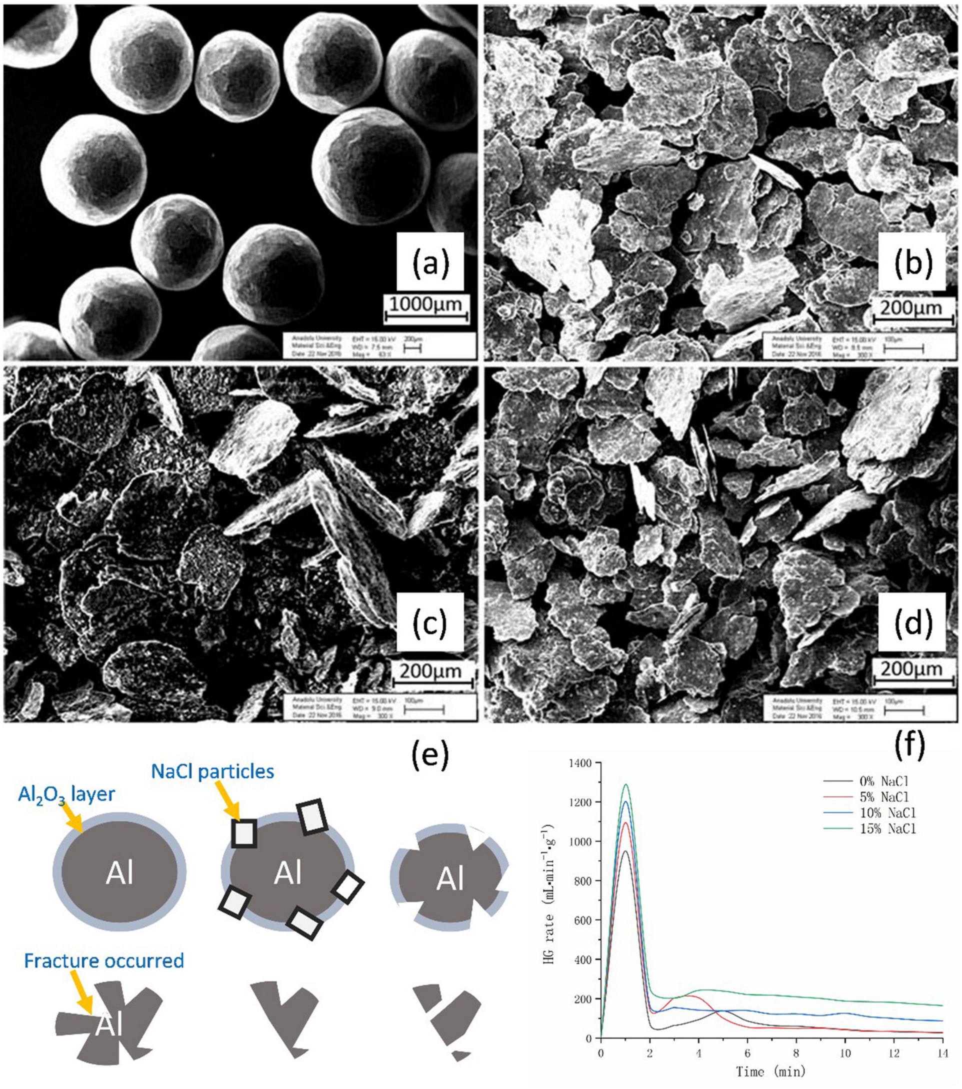

Figure 3: SEM images of the Al-NaCl powder mixtures milled for 12 h. (a) 0% NaCl, (b) 5% NaCl, (c) 10% NaCl, (d) 20% NaCl [65] (e) NaCl ball milling Al mechanism diagram; (f) Hydrogen generation rate in the reaction of water with the Al-*X* wt.% NaCl (*X* = 0, 5, 10, and 20%) powder mixture with 12 h milling time at 70°C.

on the surface, resulting in a decline in the specific surface area and consequently a decrease in the hydrogen yield. It is worth mentioning that the by-products of Co or Ni can be easily separated by their magnetic properties and reused in the subsequent hydrogen production cycle.

3.2 Oxide additives

The addition of oxide in the ball milling also directly makes close contact between aluminum powder and oxide powder and reduces the generation of the oxide film, so that the modified aluminum powder can react with water to generate hydrogen continuously.

Deng *et al.* [67] investigated the effect of different oxides (γ-Al_2O_3, α-Al_2O_3, TiO_2) on the hydrogen production rate of the Al–water reaction. After the oxide was added, the surface of the aluminum particles was covered with fine oxide particles, which were not as smooth as the original aluminum particles, as shown by the SEM and TEM micrographs in Figure 5(a–h); the hydrogen production curve is shown in Figure 5(i). Due to the low nucleation and conversion potential, the density of the oxide film of the ball-milled Al is lower than before. Consequently, the new particles can readily react with water for hydrogen production. Dupiano *et al.* [68] explored the effect of the addition of five different metal powders (MoO_3, Bi_2O_3, CuO, MgO, Al_2O_3) on the hydrogen production of the Al–water reaction. The surface structure of oxide powder additions detected by SEM is shown in Figure 5(j–n) and the hydrolysis reactions at 80°C are shown in Figure 5(o). It is obvious that Al–Bi_2O_3 has the fastest reaction rate and

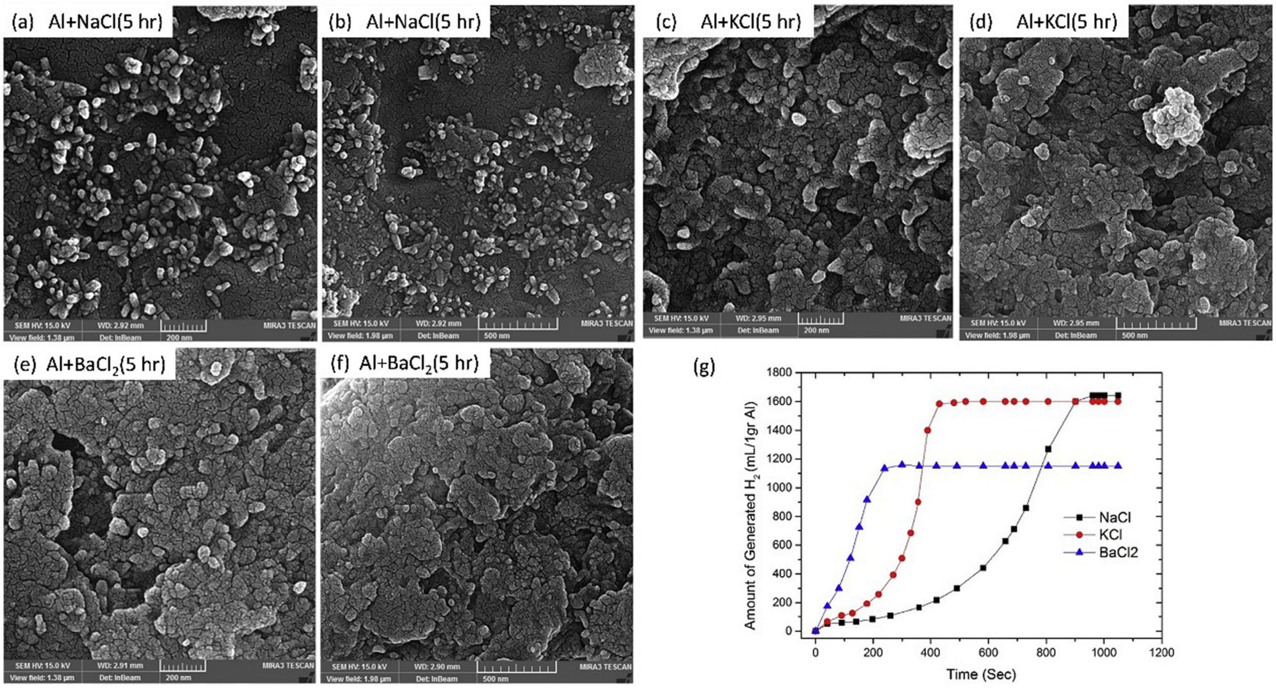

Figure 4: SEM images of 5 h ball milled Al powder with (a, b) 2 wt.% NaCl; (c, d) 2 wt.% KCl; (e, f) 2 wt.%BaCl$_2$; (g) Effect of type of salt on the hydrogen generation yield after ball milling for 5 h [66].

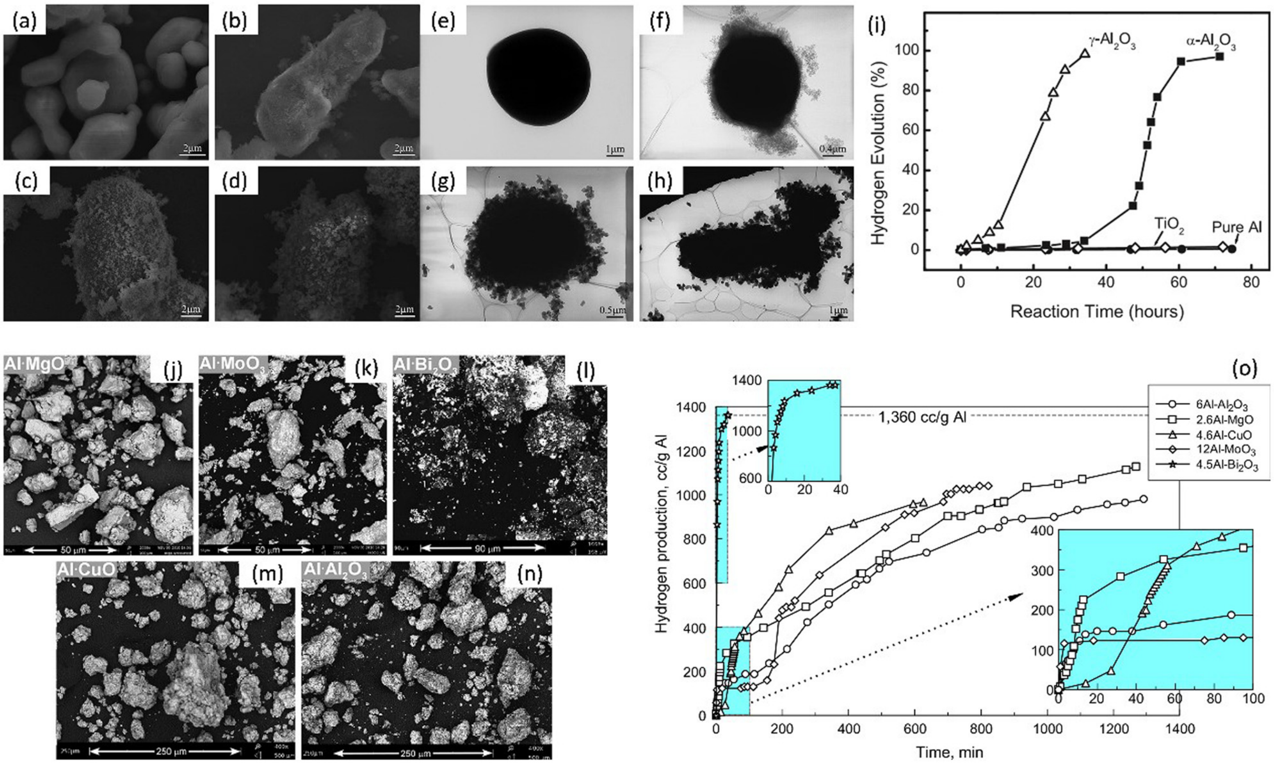

Figure 5: SEM micrographs of (a) pure Al powder and those modified by (b) g-Al$_2$O$_3$, (c) a-Al$_2$O$_3$ and (d) TiO$_2$ grains (e–h) TEM micrographs of the composition of 70 vol% Al+30 vol% oxide(e) pure Al powder (f) γ-Al$_2$O$_3$, (g) α-Al$_2$O$_3$ (h) TiO$_2$ (i) Hydrogen production curve of 70 vol% Al+ 30 vol% oxide at 22°C [67] (j–n) SEM images of different oxide additions; (o) Hydrogen production for different composites reacting with water at 80°C [68].

Table 1: A summary of ball-milled binary Al composites

Composite (wt%)	Reaction temperature (°C)	Hydrogen yield (%)	Ref.
Al–10 wt% In	90	<15	[69]
Al–23 wt% Bi	Room temperature	~80	[70]
Al–10 wt% Bi	35	81	[71]
Al–10 wt% Sn	35	74	[71]

the highest hydrogen yield. In addition, an interesting phenomenon was found during the reaction of Bi_2O_3. The reaction would stop when the experimental temperature was lowered to room temperature, and the generation rate returned to the original when the temperature was 80°C.

3.3 Addition of low melting point metals

The advantages of adding the low melting point metals to ball-milled aluminum are as follows: (1) discontinuous oxide film on the aluminum surface; (2) higher energy potential of the melting point metal than that of aluminum, and galvanic cell corrosions occur in water; and (3) prohibition of the production of $Al(OH)_3$ on the aluminum surface.

3.3.1 Binary Al composites

From Table 1, it is evident that Bi and Sn worked as active metals for binary Al composites. Nevertheless, the hydrogen yield from binary Al composites is low (85%)

Table 2: A summary of ball-milled ternary Al composites

Activation metals	Composite (wt%)	Reaction temperature (°C)	Hydrogen yield (%)	Ref.
Bi–Sn	Al–9Bi–1Sn	Room temperature	99	[72]
	Al–7.5Bi–2.5Sn	Room temperature	99	[72]
	Al–5Bi–5Sn	Room temperature	99	[72]
	Al–2.5Bi–7.5Sn	Room temperature	38.5	[72]
	Al–4.5Bi–0.5Sn	Room temperature	99	[72]
	Al–3.75Bi–1.25Sn	Room temperature	98	[72]
	Al–2.5Bi–2.5Sn	Room temperature	99	[72]
	Al–7.5Bi–2.5Sn	35	86	[71]
	Al–5Bi–5Sn	35	84	[71]
Bi-In	Al–8.38Bi–4.71In	Room temperature	95	[73]
	Al–9.38Bi–0.62In	Room temperature	81.5	[74]
	Al–8.76Bi–1.26In	Room temperature	82.5	[74]
	Al–7.5Bi–2.5In	Room temperature	95.5	[74]
	Al–5Bi–5In	Room temperature	93	[74]
	Al–3.74Bi–6.26In	Room temperature	77	[74]
	Al–2.5Bi–7.5In	Room temperature	93	[74]
	Al–1.26Bi–8.76In	Room temperature	~65	[74]
	Al–0.62Bi–9.38In	Room temperature	0	[74]
In-Sn	Al–2.54In–10.55Sn	Room temperature	93	[73]
	Al–9.82In–3.27Sn	Room temperature	93	[73]
	Al–1In–3Sn	60	11.91	[75]
	Al–3In–3Sn	Room temperature	15	[76]
	Al–3In–5Sn	Room temperature	16	[76]
	Al–3In–7Sn	Room temperature	18	[76]
	Al–3In–10Sn	Room temperature	19	[76]
	Al–0.5In–9.5Sn	Room temperature	25	[77]
	Al–2In–8Sn	Room temperature	97	[77]
	Al–3.5In–6.5Sn	Room temperature	96	[77]
	Al–5In–5Sn	Room temperature	99	[77]
	Al–6.5In–3.5Sn	Room temperature	97	[77]
	Al–8In–2Sn	Room temperature	91	[77]
	Al–9.5In–0.5Sn	Room temperature	0	[77]
	Al–1In–4Sn	Room temperature	63	[77]
	Al–1.75In–3.25Sn	Room temperature	75	[77]
	Al–2.5In–2.5Sn	Room temperature	83	[77]
	Al–3.25In–1.75Sn	Room temperature	71	[77]

Table 3: A summary of quaternary and quinary ball milled Al composites

Activation metals	Composite (wt%)	Reaction temperature (°C)	Hydrogen yield (%)	Ref.
Ga–In–Sn	Al–3Ga–3In–3Sn	Room temperature	88	[76]
	Al–3Ga–3In–5Sn	Room temperature	99	[76]
	Al–3Ga–3In–7Sn	Room temperature	68	[76]
	Al–3Ga–3In–10Sn	Room temperature	68	[76]
	Al–1Ga–1In–2Sn	60	14.71	[75]
Bi–In–Sn	Al–3.93Bi–3.93In–5.24Sn	Room temperature	91.2	[73]
	Al–6.54Bi–3.93In–2.62Sn	Room temperature	Approximately 93	[73]
	Al–3.93Bi–6.54In–2.26Sn	Room temperature	98	[73]
	Al–3.93Bi–2.62In–6.54Sn	Room temperature	Approximately 95	[73]
Bi–Ga–Zn	Al–10Bi–8Ga–2Zn	Room temperature	47	[78]
	Al–10Bi-2Ga–8Zn	Room temperature	66	[78]
	Al–10Bi–5Ga–5Zn	Room temperature	80	[78]
	Al–8Bi–2Ga–10Zn	Room temperature	76	[78]
	Al–2Bi–8Ga–10Zn	Room temperature	0	[78]
	Al–5Bi–5Ga–10Zn	Room temperature	68	[78]
	Al–2Bi–10Ga–8Zn	Room temperature	0	[78]
	Al–8Bi–10Ga–2Zn	Room temperature	16	[78]
	Al–5Bi–10Ga–5Zn	Room temperature	86	[78]

and the amount of active metal added is comparably high with large consumption.

3.3.2 Ternary Al composites

By the hydrolysis performance of Bi and Sn in binary composites, researchers started to investigate different ratios of Al–Bi–Sn alloys. Table 2 shows some of the recent articles on ternary composites. The hydrogen yield of Al–Bi–Sn alloys with a 5 wt% (Bi + Sn) content is close to the theoretical values at room temperature. Even with the same composition of the material, different ball milling procedures (ball milling time, ball-to-powder ratio) displayed different hydrogen production performances. Microstructures show that Bi and Sn promote structural disruption of Al during the mechanochemical treatment, which easily reduces the size of Al particles. Bi and Sn are relatively uniformly distributed throughout the Al particles promoting the galvanic cell reaction between the Al and Bi/Sn during the Al–water reaction.

In addition, researchers also investigated the effect of ball milling on Al–Bi–In and Al–In–Sn powders. As shown in Table 1, the Al–In mixture is essentially non-hydrolytic with water. However, Al–In–Sn powders show good hydrolysis after the gradual replacement of a portion of In with Sn. The hydrogen yield of Al–7.5Bi–2.5In powders is close to the theoretical values. Hence, Bi and In were completely dispersed on the aluminum surface, destroying the protective layer on the aluminum surface which is different from Bi–Sn. Unlike the previous two composites, Al–In–Sn formed new phases during ball milling – In_3Sn and $InSn_4$. Nearly 100% hydrogen yield was achieved with Al–5In–5Sn.

Taking into account the costs of the raw material, ternary Al–Bi–Sn powder is a particularly suitable choice, and with a suitable ball milling process, excellent hydrogen production can be achieved for practical applications in future.

3.3.3 Quaternary and multiple Al composites

The progress of hydrogen production performance of quaternary Al composites is summarized in Table 3. It can be seen that the hydrogen production performance of the quaternary Al composite is excellent, whereas it has no obvious advantage over the ternary Al composites, and it is more difficult to recover the fourth-series Al composites due to their complexity.

3.4 Other additives

The effects of additions of different mixtures on the hydrolysis effect of the composite have been analyzed. Wu *et al.* [79] prepared Al–10 mol% CaH_2–10 mol% $NiCl_2$ and it gave a hydrogen yield of 92.1% at 75°C with a maximum hydrogen generation rate of 1566.3 mL/(g min) after 3 h ball milling. The hydrolysis process leads to the formation of a new compound $Ca_2Al(OH)_6Cl(H_2O)_2$, which stimulates to remove the dense by-product layer. Liu *et al.* [80] developed a mixture of Al and Li_3AlH_6 which gave 92.8% of hydrogen yield at room temperature. Chen *et al.* [81] added 5 wt% NaCl during ball milling of Al–10 wt% $Bi(OH)_3$, and the hydrogen generation rate elevated to 1,000 mL/(g min) at 30°C. Liao *et al.* [82] prepared Al–5wt%Bi@C and achieved 36% hydrogen yield at 60°C; the SEM micrographs are shown in Figure 6(a) and (b). On the contrary, when sintered in a plasma discharge sintering furnace, the product of blocks gave 100% theoretical hydrogen yield, as shown in Figure 6(c). Also, the sintered material reflects excellent oxidation resistance and still displays a 75.5% hydrogen yield after being exposed to air for 30 days. The main reason is that the number of carbon defects and cracks increased by the sintering process on the surface of the block. The effect of different processing methods on the surface microstructure of the Al–Bi@C material is shown in Figure 6(d and e). As shown in Figure 6(f), the intensity ratio of the D band to the G band (ID/IG) is 0.948 for Al–Bi@C milled and 0.952 for Al–Bi@C SPS. This indicates that ball milling increases the carbon defects and the SPS process further enhances carbon defects, which helps to improve the reactivity of the block. In particular, the sintering process not only increases the hydrogen generation rate of Al composites but also improves its oxidation resistance. Therefore, this method is expected to have practical uses in the field of hydrogen supply.

Generally, aluminum powder composites prepared by ball milling had the advantages of high hydrogen yield, high hydrogen generation rate, and short reaction induction time. The higher the activity, the higher the requirements for preparation, transportation, and storage. However, its short storage time is an obvious disadvantage. Furthermore, the high cost and time-consuming ball milling procedure is another obstacle not suitable for large-scale processing. Nonetheless, it cannot be overlooked that the high activity provided by the ball-milled aluminum powder can provide a large amount of hydrogen swiftly in an emergency and has a wide range of prospects for commercial application.

4 Low melting point metal-activated aluminum alloys

4.1 Block alloys

When hydrargyrum is dropped on the aluminum plate where the oxide film has just been removed, tall blocks will gradually grow on the aluminum plate. As shown in Figure 7(a–c), it was found that hydrargyrum can help the

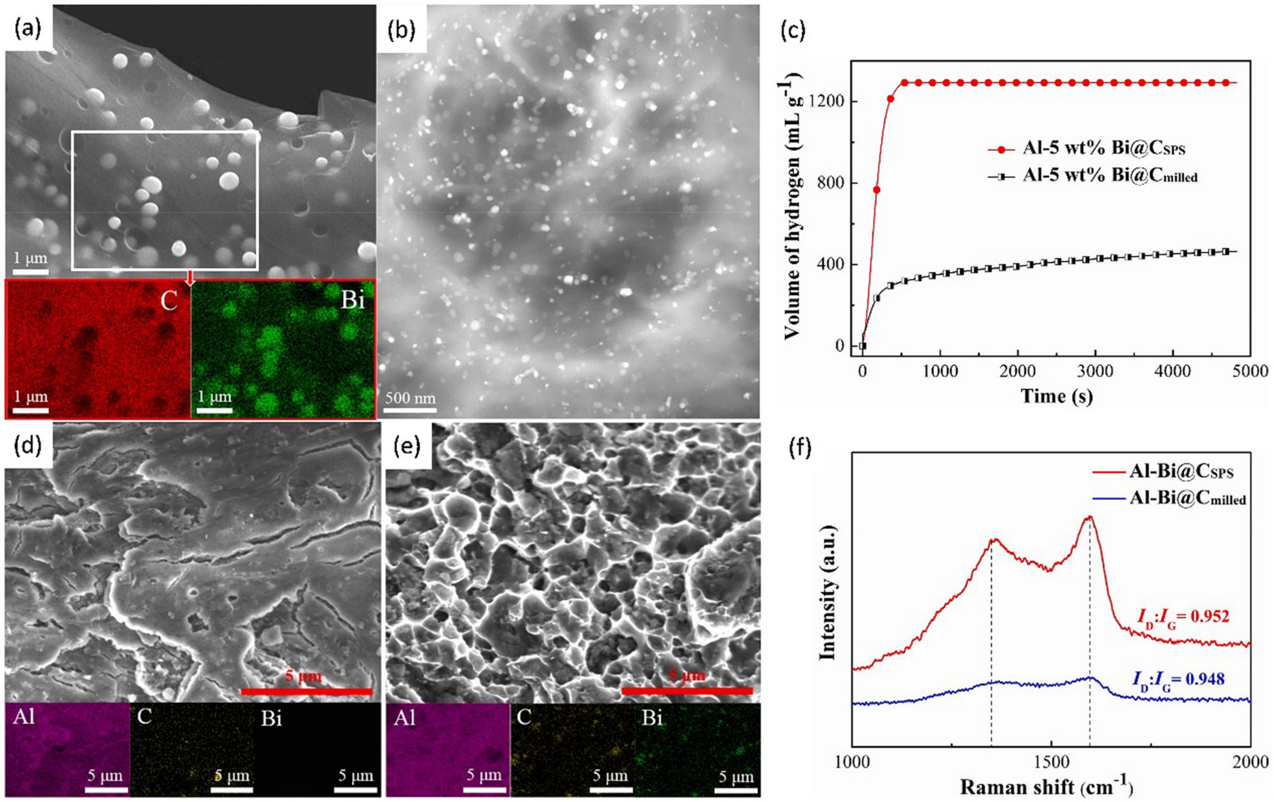

Figure 6: SEM-EDS (a) and TEM (b) images of Bi@C; SEM-EDS images of (c) Al-Bi@C milled and (d) Al-Bi@C SPS; (e)Raman spectra of Al–Bi@C SPS and Al–Bi@C milled; (f) Hydrogen generation curves for Al-5 wt.% Bi@C milled and Al-5 wt.% Bi@C SPS [82].

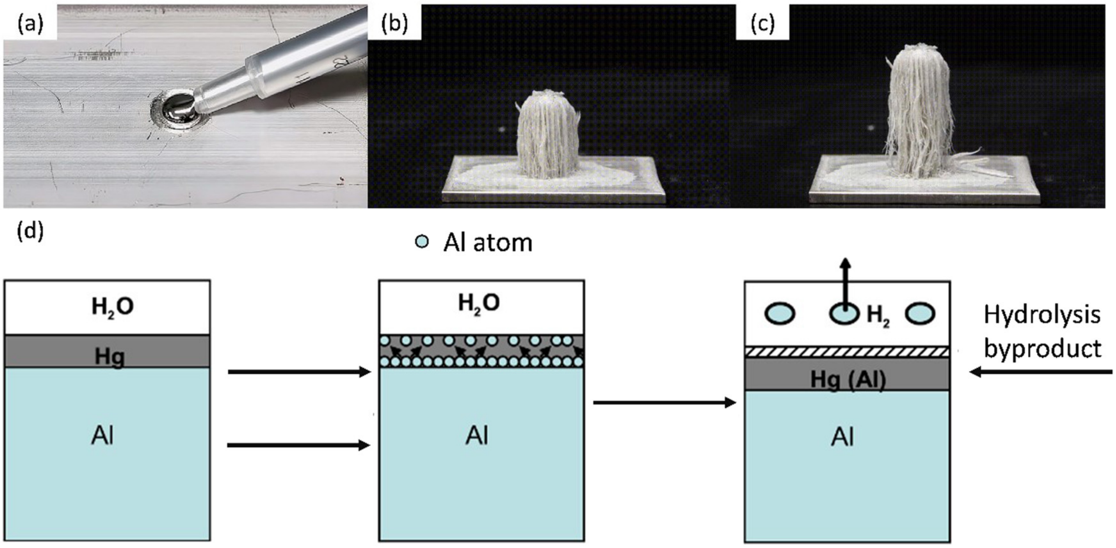

Figure 7: Proposed aluminum hydrolysis model induced by mercury [83].

hydrolysis reaction to produce hydrogen from aluminum that has just been removed from the oxide film at 65°C [83]. The main reason is hydrargyrum stops the regeneration of the aluminum oxide film. The reaction is shown in Figure 7(d). Similarly, Woodall *et al.* [84] first prepared different compositions of Al–Ga liquid alloys which can react with water and produce hydrogen at room temperature. After the dissolution of low melting point metals, the Al_2O_3 layer become discontinuous and porous, which indeed improved the activities of the Al matrix. Thus, the effects of other low melting point metals (Li, Bi, In, Sn, Mg, *etc.*) on the hydrogen production from the Al–water reaction were investigated below.

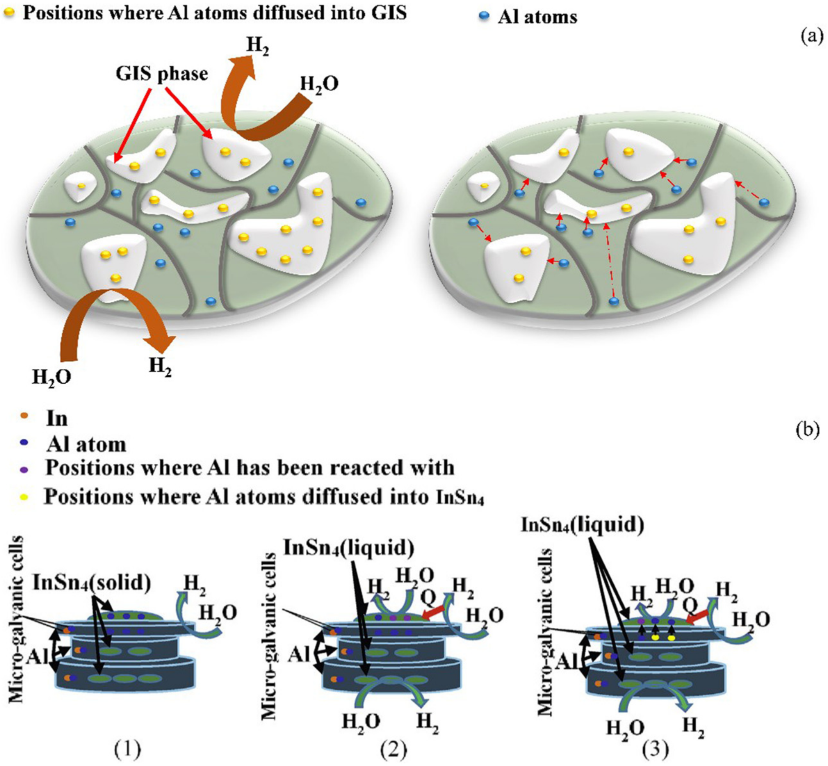

Figure 8: Diagram of hydrolysis reaction mechanism of hydrolysis Al-Ga-In-Sn alloys (a); (b) [90].

4.1.1 Binary and ternary Al alloys

Woodall *et al.* [85] found that Al–72 wt% Ga and Al–50 wt% Ga show hydrolysis at 26–27°C, which is clearly due to the melting point of the Al (Ga) solid solution (about 26.6°C). Along with the hydrolysis reaction process and temperature, Ga dissolves in the Al matrix which does not participate in the reaction and only acts as an active component similar to a catalyst. Nevertheless, the hydrogen yield of Al–Ga alloys is deficient, which cannot satisfy the practical requirements. The emergence of binary alloys provides us with the possibility of hydrogen generation from the Al–water reaction but the hydrogen yield is low and the amount of a single precious metal is too large to be suitable for general applications. Otherwise, Al–Ga alloys not only display lower hydrogen production efficiency but also exhibit mechanical brittleness. In particular, Zhou *et al.* [86,87] verified this conclusion by first-principles calculations and found that the solid solution of Ga significantly reduces the strong toughness of the aluminum matrix. Al–Ga alloys are observed to produce H_2 at a reaction temperature of about 26°C which is close to the melting point of Al–Ga eutectic. Therefore, lowering the melting point of the low melting point phase in the alloy to reduce the initial reaction temperature is an important idea. He *et al.* [88] investigated the reactivity of Al–Ga–In and Al–Ga–Sn alloys with water. The heat absorption peaks of Al–Ga–In and Al–Ga–Sn appear at 15°C and 19°C, respectively, as shown by DSC, which basically coincide with the melting points of Al–Ga–In and Al–Ga–Sn eutectics of 15.3 and 20.5°C, respectively. It was found that the Al–Ga–In alloys showed reactivity at about 10°C and the Al–Ga–Sn alloys started to show reactivity at 20°C. The reason for this is that the aluminum–-water reaction is exothermic, so the reaction temperature is slightly below the melting point. The 15 wt% (Ga + In) Al–Ga-In alloys have a hydrogen yield of more than 90% in water at 20°C. In comparison, the hydrogen yield of the 15 wt% (Ga + Sn) Al–Ga–Sn is only 12%. Although the hydrogen yield of the Al–Ga–In alloys is much higher than that of Al–Ga–Sn alloys, the hydrogen generation rate is lower than Al–Ga–Sn alloys. In general, the low melting point phase determines the starting temperature of the hydrolysis reaction, and the initial temperature at which the reaction point begins to occur follows the melting point Al–Ga–In < Al–Ga–Sn < Al–Ga, and the different compositions seriously affect the H_2 generation rate and H_2 yield. In addition, there is micro-galvanic cell corrosion in the aluminum–water reaction of the alloys, which means that the difference between Ga, In, and Sn and Al also affects the hydrogen generation rate. Consequently, further research is needed to develop alloys that combine hydrogen generation rates, hydrogen yields, and lower reaction temperatures.

4.1.2 Quaternary and multi-alloys

Wang *et al.* [89] observed the Al–Ga–In–Sn alloys showed a heat absorption peak at 11.2°C by the DSC test, slightly above the melting point of 10.7°C for Ga–In–Sn eutectic. When the mass ratio of In/Sn is equal to 1.5:0.7, the In_3Sn phase appears, and when the mass ratio is equal to 1:1, not only the In_3Sn phase but also the $InSn_4$ phase appears in the alloys. du Preez and Bessarabov [77] further observed that the formation of In and Sn intermetallic phases is determined by the molar ratio of In/Sn and In_3Sn was the dominant In–Sn phase in composites with an In/Sn ratio of <0.97.

The principle of hydrogen production in Al–Ga–In–Sn alloys is mainly based on the fact that the addition of low melting point metals generates eutectic phases with very low melting points (In_3Sn, $InSn_4$), and even though most Ga dissolves in Al, trace amounts of Ga dissolve in the InSn eutectic phase, forming a Ga–In–Sn eutectic phase (named GIS phase). The GIS phase also dissolves a certain amount of Al atoms, completely surrounding these Al atoms. Al atoms react preferentially with water, even if the Al atoms in the eutectic phase have completed reacting. They will be supplemented by Al atoms with increased activity due to the solid solution of Ga and continue to undergo hydrolysis reactions. The low melting point phase not only protects the solid-solution Al atoms from oxidation but also provides a channel for the Al atoms to diffuse to the reaction sites [91]; these lower melting point “channels” allow the alloys to react with water at lower temperatures. The reaction mechanisms of the alloys are shown in Figure 8. In order to produce larger amounts of H_2, it is necessary to maintain a suitable number of “channels” and the eutectic phase must be small and uniformly distributed [92,93]. If the channels are too small, the activation energy will be reduced, thereby slowing down the hydrolysis reaction and reducing the hydrogen generation rate. If the channels are too large, at the same time, the content of rare and precious metals will increase, which will increase the cost. Only when the low melting point eutectic phase is uniformly and finely distributed on the surface of the aluminum substrate can all the aluminum be activated to the maximum.

Al–Ga–In–Sn alloys have excellent hydrogen production properties, and researchers added other metals (Bi, Zn, Cu, Mg, Li) or compounds (Al_2O_3, Al–5Ti–B) to achieve

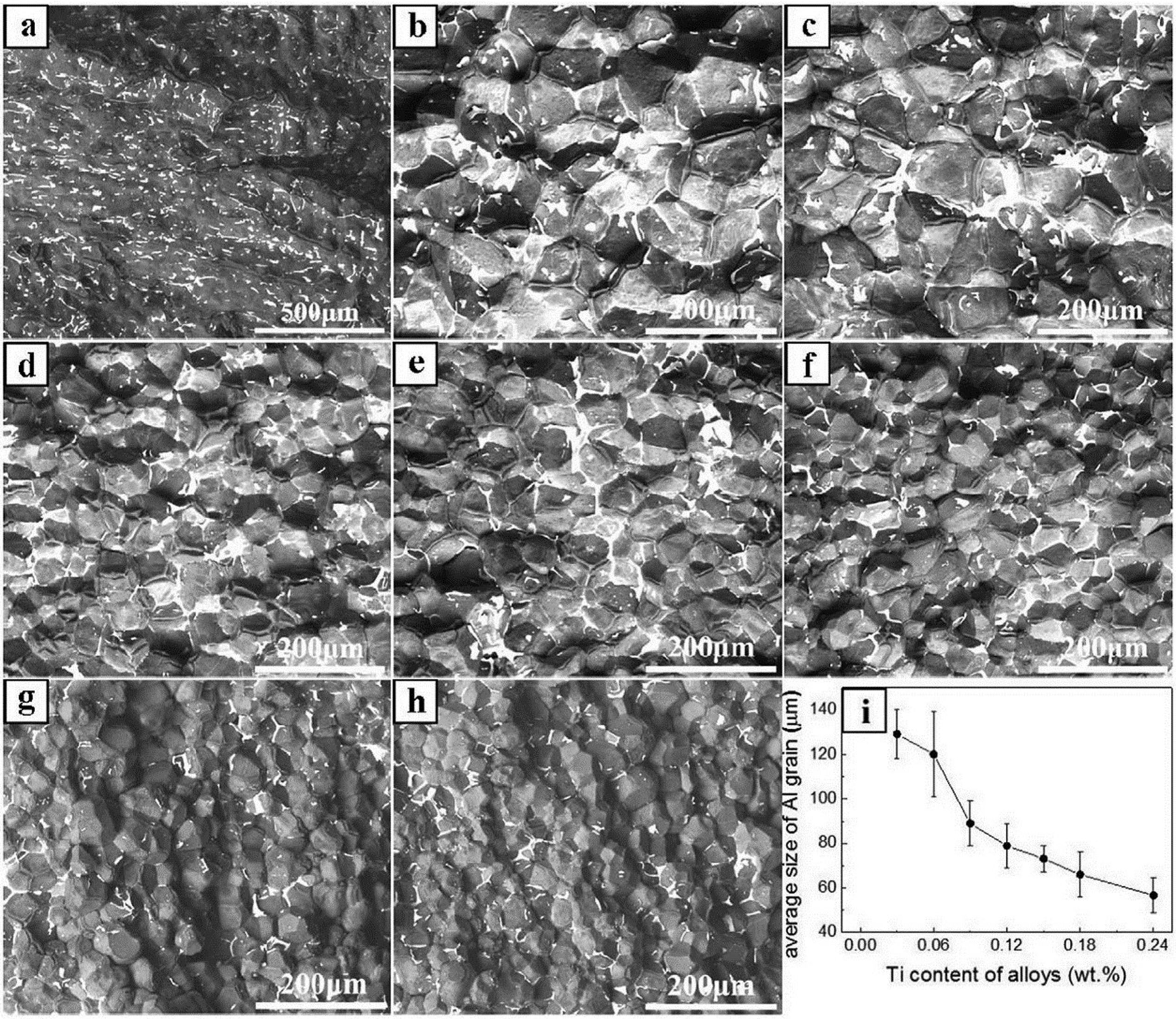

Figure 9: The fracture surfaces of 6 wt.% Al-Ga-In-Sn alloys with different Ti contents and relations of Al grain size with Ti contents: (a) Ti free, (b) Ti 0.03 wt.%, (c) Ti 0.06 wt.%, (d) Ti 0.09 wt.%, (e) Ti 0.12 wt.%, (f) Ti 0.15 wt.%, (g) Ti 0.18 wt.%, (h) Ti 0.24 wt.%, (i) relations of Al grain size with Ti contents [98].

one or more goals of cost reduction, reaction rate modulation. and strength increase. Ga and In are expensive, so the proportion of their use needs to be kept as low as possible. Huang *et al.* [94] added Bi to 80 wt% Al–Ga–In–Sn alloys to replace In, compared with the Al–Ga–In–Sn alloys, the hydrogen generation rate was smooth and controllable, and the hydrogen yield could reach the theoretical value. An *et al.* [95] increased the Al content to 90 wt% on this basis, and the hydrogen yield at 40°C was already close to 100%, with a maximum hydrogen generation rate of 780 mL/(g min). Wei *et al.* [96] explored the effect of partial substitution of $InSn_4$ with Cu on the hydrogen production effect and found that the hydrogen yield and hydrogen generation rate of Al–Ga–$InSn_4$–Cu alloy ingots with 3 wt% Cu content were better than Al–Ga–$InSn_4$ alloys.

Along with an increase in the hydrogen yield, the hydrogen generation rate in the alloys needs to be regulated. Wei *et al.* [97] replaced Al in the Al–Ga–In_3Sn alloys

Table 4: Effect of adding different materials to Al–Ga–In–Sn alloys

Materials	Refining grain	Slows down the generation rate	Increase yields
Bi		√	
Zn		√	
Cu	√	√	√
Mg	√	√	
Li		√	
Al_2O_3		√	√
Al–5Ti–B	√		√

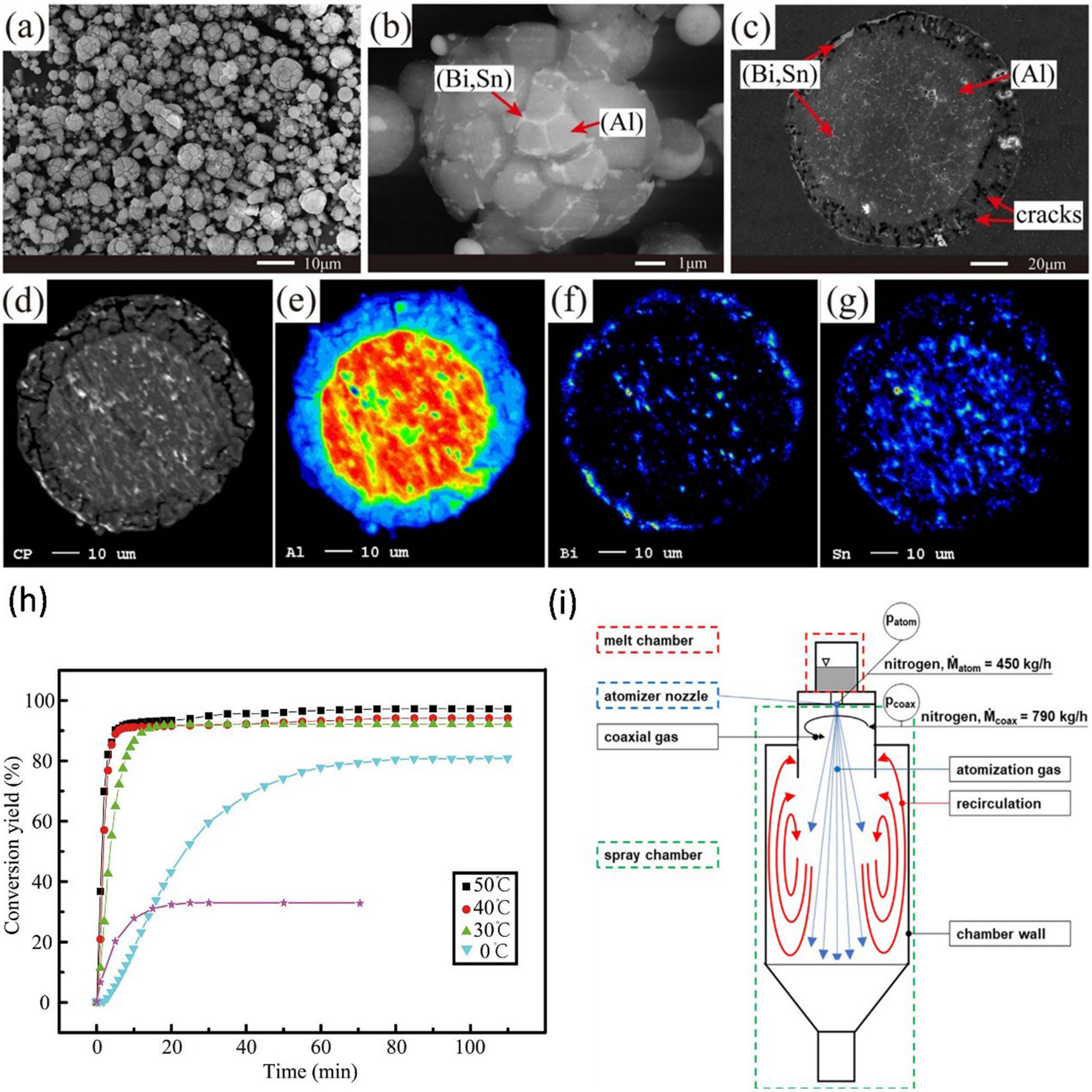

Figure 10: (a–c) SEM images of the 80Al-10Bi-10Sn wt. % powders: (a, b) surfaces, (c) cross-section; (d–g) EPMA element mappings of the cross section of the powders: (d) BSE, (e) Al, (f) Bi, and (g) Sn. (h) Hydrogen generation curves of the 80Al-10Bi-10Sn wt.% powders in distilled water [106] (i) A typical gas atomization device [107].

with Al_2O_3 and found that 1 wt% Al_2O_3 contributed to the raised hydrogen generation rate of the alloys but had no effect on the hydrogen yield. Grain refinement is an important method to enhance the hydrogen generation rate. Du *et al.* [98] added 0.12 wt% Al–5Ti–B to Al–Ga–In–Sn alloys; the grain size was reduced from 129 to 57 μm, as shown in Figure 9, and the alloys achieved 87% H_2 yield at 30°C. Wei *et al.* [97] found that replacing In and Sn with Al_2O_3 can slow down the hydrogen generation rate of the alloys but has little effect on the hydrogen yield. He *et al.* [99] prepared Al–Ga–In–Sn–Li alloys with different Li contents. On increasing the Li content, the hydrogen generation rate of the alloys decreased significantly, while the hydrogen yield decreased slightly. Liu *et al.* [100] investigated the effect of Zn by replacing some of In_3Sn on the hydrogen production properties of the Al–Ga–In_3Sn alloys and realized that at 2 wt% Zn content, the hydrogen generation rate of the alloys decreased significantly compared to the hydrogen generation rate of the alloys without Zn. While the presence of Zn in the alloys is similar to that of Ga, mainly in the form of Al–Zn solid solution, it can retard the peak hydrogen generation rate mainly due to the formation of an Al–Zn micro-galvanic cell. In addition, Cu and Mg can effectively slow down the hydrogen generation rate but have less effect on the hydrogen yield [101–104].

Soluble materials are critical in horizontal well fracturing technology for unconventional oil and gas field development. The water-soluble nature of the alloys allows them to be used as a downhole soluble fracturing material, subject to compressive performance requirements. With the addition of Cu and Mg, the Al grain size becomes significantly finer and the strength of the Al–Ga–In–Sn alloys increases [101–103]. The functions of the different materials are summarized in Table 4.

4.2 Gas-atomized alloys

The gas atomization process is a widely used powder manufacturing process that offers good uniformity and the possibility of mass production. It is a process in which a high-speed, high-pressure media flow is generated by an atomizing nozzle to crush the molten metal into fine droplets, which are subsequently spherified, cooled, and solidified into a metal powder. In addition, gas atomization is more suitable for mass production than ball milling [105].

As previously mentioned, ball-milled Al–Bi–Sn composites reflected high H_2 yield and H_2 generation rates, yet this composite cannot be prepared by melting because it is a difficult miscible alloy that can easily cause solid–liquid separation. Wang *et al.* [106] prepared Al–10wt%Bi–10wt% Sn powder by gas atomization and the powder showed outstanding hydrogen generation performance, with 80.4% H_2 yield at 0°C for 88 min and 91.3% at 30°C for 16 min with water. Liu *et al.* [108] prepared Al–20wt%Bi powder with a core–shell structure, as shown in Figure 10(a–g). The powder reacted at room temperature and reached 100% theoretical H_2 yield, as shown in Figure 10(h).

The composite powder prepared by gas atomization has a significant H_2 generation rate at low temperatures and the process is simpler than ball milling. However, the disadvantages are similar to ball milling, which can lead to unsafe storage and short storage times.

5 Conclusions

Hydrogen, with its high calorific value, low density, and only water as a combustion product is a promising renewable energy source. Nevertheless, there are safety risks in storage and transport, so there is a need to develop a safe, environmentally friendly, and portable hydrogen energy application. Hydrolysis of aluminum-based materials can improve this role. Surface passivation of aluminum in air remains a major obstacle to the reaction of aluminum with water and this study provides a detailed review of the main methods for removing Al_2O_3 or destroying it from aluminum surfaces:

1) The reaction of aluminum with acid–alkali solutions is the simplest principle of hydrogen production and has high requirements for experimental equipment.
2) Ball milling of aluminum powder can produce hydrogen quickly and is suitable for rapid hydrogen production under emergency conditions, but extra attention should be paid to the safety hazards and short storage time of aluminum powder as well as the time and cost of ball milling.
3) The melting and casting have the advantages of a simple process, low cost, high efficiency, and easy factory mechanization that are difficult to replace. Although the hydrogen yield and the hydrogen generation rate are lower than ball milling, it has the additional advantage of long storage times under dry conditions.
4) The gas materialization adds a process to turn the solute into a powder when casting. The properties of the powder are close to powder prepared by ball milling, and advantages are similar to those of the ball milling, with poorer safety and shorter storage times.

In brief, Al-based materials have been successfully used in mobile hydrogen production equipment, hydrogen fuel cells, and other fields, and it has wide application prospects in many fields. For Al-based materials to have a better commercial future, there are still some issues that need continued attention:

1) As the alloys are water-soluble and can be strengthened by adding reinforcing metals, other scenarios have been developed for use and for developing applications for a wider range of use environments.
2) In order to improve energy efficiency and reduce raw material costs, the use of high-purity aluminum is gradually being replaced by scrap aluminum or industrial pure aluminum.
3) For cost and environmental considerations, the focus should be on scientific research and analysis in terms of by-product analysis, collection, and reuse.

Funding information: This work was supported by the Key Research and Development Program of Shaanxi (Program

No. 2022QCY-LL-58), the Natural Science Basic Research Plan in Shaanxi Province of China (2023-JC-YB-458), Science and Technology Project of Huaneng Group Co, Ltd. (HNKJ 20-H41), and the Graduate Student Innovation and Practical Ability Training Program of Xi'an Shiyou University (YCS20212116).

Author contributions: All authors have accepted responsibility for the entire content of this manuscript and approved its submission.

Conflict of interest: The authors state no conflict of interest.

References

[1] Sutrisno A, Nomaler Ö, Alkemade F. Has the global expansion of energy markets truly improved energy security? Energy Policy. 2021;148:111931.

[2] Kivimaa P, Sivonen MH. Interplay between low-carbon energy transitions and national security: An analysis of policy integration and coherence in Estonia, Finland and Scotland. Energy Res Soc Sci. 2021;75:102024.

[3] Derse O, Göçmen E, Yılmaz E, Erol R. A mathematical programming model for facility location optimization of hydrogen production from renewable energy sources. Energy Sources Part A: Recov Util Environ Eff. 2022;44(3):6648–59.

[4] Yao Y, Gao X, Meng X. Recent advances on electrocatalytic and photocatalytic seawater splitting for hydrogen evolution. Int J Hydrogen Energy. 2021;46(13):9087–100.

[5] Londoño-Pulgarin D, Cardona-Montoya G, Restrepo JC, Muñoz-Leiva F. Fossil or bioenergy? Global fuel market trends. Renew Sustain Energy Rev. 2021;143:110905.

[6] Zanganeh KE, Shafeen A. A novel process integration, optimization and design approach for large-scale implementation of oxy-fired coal power plants with CO2 capture. Int J Greenh Gas Control. 2007;1(1):47–54.

[7] Pareek A, Dom R, Gupta J, Chandran J, Adepu V, Borse PH. Insights into renewable hydrogen energy: Recent advances and prospects. Mater Sci Energy Technol. 2020;3:319–27.

[8] Moreira dos Santos R, Szklo A, Lucena AFP, de Miranda PEV. Blue sky mining: Strategy for a feasible transition in emerging countries from natural gas to hydrogen. Int J Hydrogen Energy. 2021;46(51):25843–59.

[9] Maggio G, Nicita A, Squadrito G. How the hydrogen production from RES could change energy and fuel markets: A review of recent literature. Int J Hydrogen Energy. 2019;44(23):11371–84.

[10] Kötter E, Schneider L, Sehnke F, Ohnmeiss K, Schröer R. The future electric power system: Impact of Power-to-Gas by interacting with other renewable energy components. J Energy Storage. 2016;5:113–9.

[11] Colbertaldo P, Agustin SB, Campanari S, Brouwer J. Impact of hydrogen energy storage on California electric power system: Towards 100% renewable electricity. Int J Hydrogen Energy. 2019;44(19):9558–76.

[12] Kovač A, Paranos M, Marciuš D. Hydrogen in energy transition: A review. Int J Hydrogen Energy. 2021;46(16):10016–35.

[13] Vincent I, Bessarabov D. Low cost hydrogen production by anion exchange membrane electrolysis: A review. Renew Sustain Energy Rev. 2018;81:1690–704.

[14] Balat M. Potential importance of hydrogen as a future solution to environmental and transportation problems. Int J Hydrogen Energy. 2008;33(15):4013–29.

[15] Banerjee S, Musa MN, Jaafar AB. Economic assessment and prospect of hydrogen generated by OTEC as future fuel. Int J Hydrogen Energy. 2017;42(1):26–37.

[16] Kler AM, Tyurina EA, Potanina YM, Mednikov AS. Estimation of efficiency of using hydrogen and aluminum as environmentally-friendly energy carriers. Int J Hydrogen Energy. 2015;40(43):14775–83.

[17] Hosseini SE, Wahid MA. Hydrogen production from renewable and sustainable energy resources: Promising green energy carrier for clean development. Renew Sustain Energy Rev. 2016;57:850–66.

[18] Yu M, Kim M, Yoon B, Oh S, Nam D-H, Kwon H. Carbon nanotubes/aluminum composite as a hydrogen source for PEMFC. Int J Hydrogen Energy. 2014;39(34):19416–23.

[19] Sinigaglia T, Lewiski F, Santos Martins ME, Mairesse Siluk JC. Production, storage, fuel stations of hydrogen and its utilization in automotive applications-a review. Int J Hydrogen Energy. 2017;42(39):24597–611.

[20] Safari F, Dincer I. A review and comparative evaluation of thermochemical water splitting cycles for hydrogen production. Energy Convers Manag. 2020;205:112182.

[21] Abdalla AM, Hossain S, Nisfindy OB, Azad AT, Dawood M, Azad AK. Hydrogen production, storage, transportation and key challenges with applications: A review. Energy Convers Manag. 2018;165:602–27.

[22] Abbasi T, Abbasi SA. 'Renewable' hydrogen: Prospects and challenges. Renew Sustain Energy Rev. 2011;15(6):3034–40.

[23] Coronel-García MA, Salazar-Barrera JG, Malpica-Maldonado JJ, Martínez-Salazar AL, Melo-Banda JA. Hydrogen production by aluminum corrosion in aqueous hydrochloric acid solution promoted by sodium molybdate dihydrate. Int J Hydrogen Energy. 2020;45(26):13693–701.

[24] Parkinson B, Balcombe P, Speirs JF, Hawkes AD, Hellgardt K. Levelized cost of CO2 mitigation from hydrogen production routes. Energy Environ Sci. 2019;12(1):19–40.

[25] da Silva Veras T, Mozer TS, da Costa Rubim Messeder dos Santos D, da Silva César A. Hydrogen: Trends, production and characterization of the main process worldwide. Int J Hydrogen Energy. 2017;42(4):2018–33.

[26] Nikolaidis P, Poullikkas A. A comparative overview of hydrogen production processes. Renew Sustain Energy Rev. 2017;67:597–611.

[27] Nicoletti G, Arcuri N, Nicoletti G, Bruno R. A technical and environmental comparison between hydrogen and some fossil fuels. Energy Convers Manag. 2015;89:205–13.

[28] Gutiérrez-Martín F, García-De María JM, Baïri A, Laraqi N. Management strategies for surplus electricity loads using electrolytic hydrogen. Int J Hydrogen Energy. 2009;34(20):8468–75.

[29] Landman A, Dotan H, Shter GE, Wullenkord M, Houaijia A, Maljusch A, et al. Photoelectrochemical water splitting in separate oxygen and hydrogen cells. Nat Mater. 2017;16(6):646–51.

[30] Satyapal S, Petrovic J, Read C, Thomas G, Ordaz G. The U.S. Department of Energy's National Hydrogen Storage Project: Progress towards meeting hydrogen-powered vehicle requirements. Catal Today. 2007;120(3–4):246–56.

[31] Xiao P, Hu W, Xu X, Liu W, Huang Q, Chen Z. Optimal operation of a wind-electrolytic hydrogen storage system in the electricity/hydrogen markets. Int J Hydrogen Energy. 2020;45(46):24412–23.

[32] Shi Y, Yang A-F, Cao C-S, Zhao B. Applications of MOFs: Recent advances in photocatalytic hydrogen production from water. Coord Chem Rev. 2019;390:50–75.

[33] Durbin DJ, Malardier-Jugroot C. Review of hydrogen storage techniques for on board vehicle applications. Int J Hydrogen Energy. 2013;38(34):14595–617.

[34] Yao Q, Zhu H. Numerical simulation of hydrogen dispersion behaviour in a partially open space by a stabilized balancing domain decomposition method. Comput Math Appl. 2015;69(10):1068–79.

[35] Najjar YSH. Hydrogen safety: The road toward green technology. Int J Hydrogen Energy. 2013;38(25):10716–28.

[36] Zhao C, Xu F, Sun L, Chen J, Guo X, Yan E, et al. A novel Al BiOCl composite for hydrogen generation from water. Int J Hydrogen Energy. 2019;44(13):6655–62.

[37] Zhao C, Xu F, Sun L, Fan M, Zou Y, Chu H. Hydrogen generation by Al-based materials hydrolysis. Prog Chem. 2016;12(28):1870–9.

[38] Tan ZH, Ouyang LZ, Huang JM, Liu JW, Wang H, Shao HY, et al. Hydrogen generation via hydrolysis of Mg2Si. J Alloy Compd. 2019;770:108–15.

[39] Ma M, Yang L, Ouyang L, Shao H, Zhu M. Promoting hydrogen generation from the hydrolysis of Mg-Graphite composites by plasma-assisted milling. Energy. 2019;167:1205–11.

[40] Tan Z, Ouyang L, Liu J, Wang H, Shao H, Zhu M. Hydrogen generation by hydrolysis of Mg-Mg2Si composite and enhanced kinetics performance from introducing of MgCl2 and Si. Int J Hydrogen Energy. 2018;43(5):2903–12.

[41] Huang M, Ouyang L, Chen Z, Peng C, Zhu X, Zhu M. Hydrogen production via hydrolysis of Mg-oxide composites. Int J Hydrogen Energy. 2017;42(35):22305–11.

[42] Zhong H, Wang H, Liu JW, Sun DL, Fang F, Zhang QA, et al. Enhanced hydrolysis properties and energy efficiency of MgH2-base hydrides. J Alloy Compd. 2016;680:419–26.

[43] Ouyang LZ, Zhong H, Li ZM, Cao ZJ, Wang H, Liu JW, et al. Low-cost method for sodium borohydride regeneration and the energy efficiency of its hydrolysis and regeneration process. J Power Sources. 2014;269:768–72.

[44] An Q, Gao Q, Wang H, Wei C, Li N. Insight into the indium-related morphology transformation and application for hydrogen production of Al-rich alloys. J Alloy Compd. 2020;842:155864.

[45] Zhang C, Li H, Guo X, Li S, Zhang H, Pan X, et al. Experimental and theoretical studies on the effect of Al(OH)3 on the fire-extinguishing performance of superfine ABC dry powder. Powder Technol. 2021;393:280–90.

[46] Ramazani SAA, Rahimi A, Frounchi M, Radman S. Investigation of flame retardancy and physical–mechanical properties of zinc borate and aluminum hydroxide propylene composites. Mater Des. 2008;29(5):1051–6.

[47] Ma M-G, Zhu J-F. A facile solvothermal route to synthesis of γ-alumina with bundle-like and flower-like morphologies. Mater Lett. 2009;63(11):881–3.

[48] Ouyang L, Chen W, Liu J, Felderhoff M, Wang H, Zhu M. Enhancing the regeneration process of consumed NaBH4 for hydrogen storage. Adv Energy Mater. 2017;7(19):1700299.

[49] Zhu Y, Ouyang L, Zhong H, Liu J, Wang H, Shao H, et al. Closing the loop for hydrogen storage: Facile regeneration of NaBH4 from its hydrolytic product. Angew Chem. 2020;132(22):8701–7.

[50] Chen K, Ouyang L, Zhong H, Liu J, Wang H, Shao H, et al. Converting H + from coordinated water into H− enables super facile synthesis of LiBH 4. Green Chem. 2019;21(16):4380–7.

[51] Guerrero SE, Dreizin EL, Shafirovich E. Combustion of thermite mixtures based on mechanically alloyed aluminum–iodine material. Combust Flame. 2016;164:164–6.

[52] Chai YJ, Dong YM, Meng HX, Jia YY, Shen J, Huang YM, et al. Hydrogen generation by aluminum corrosion in cobalt (II) chloride and nickel (II) chloride aqueous solution. Energy. 2014;68:204–9.

[53] Wang H, Wang Z, Shi Z, Gong X, Cao J, Wang M. Facile hydrogen production from Al-water reaction promoted by choline hydroxide. Energy. 2017;131:98–105.

[54] Fan MQ, Sun LX, Xu F. Experiment assessment of hydrogen production from activated aluminum alloys in portable generator for fuel cell applications. Energy. 2010;35(7):2922–6.

[55] Wang HZ, Leung DYC, Leung MKH, Ni M. A review on hydrogen production using aluminum and aluminum alloys. Renew Sustain Energy Rev. 2009;13(4):845–53.

[56] Takehito H, Masato T, Hisa M, Akitama T. Hydrogen Production from Waste Aluminum at Different Temperatures. Mater Trans. 2005;46(5):1052–7.

[57] Soler L, Macanás J, Muñoz M, Casado J. Aluminum and aluminum alloys as sources of hydrogen for fuel cell applications. J Power Sources. 2007;169(1):144–9.

[58] Aleksandrov YA, Tsyganova EI, Pisarev AL. Reaction of aluminum with dilute aqueous NaOH solutions. Russian J Gen Chem. 2003;73(5):689–94.

[59] Ambaryan GN, Vlaskin MS, Dudoladov AO, Meshkov EA, Zhuk AZ, Shkolnikov EI. Hydrogen generation by oxidation of coarse aluminum in low content alkali aqueous solution under intensive mixing. Int J Hydrogen Energy. 2016;41(39):17216–24.

[60] Alinejad B, Mahmoodi K. A novel method for generating hydrogen by hydrolysis of highly activated aluminum nanoparticles in pure water. Int J Hydrogen Energy. 2009;34(19):7934–8.

[61] Avar B, Ozcan S. Structural evolutions in Ti and TiO2 powders by ball milling and subsequent heat-treatments. Ceram Int. 2014;40(7):11123–30.

[62] Raghavendra KG, Dasgupta A, Bhaskar P, Jayasankar K, Athreya CN, Panda P, et al. Synthesis and characterization of Fe-15 wt% ZrO2 nanocomposite powders by mechanical milling. Powder Technol. 2016;287:190–200.

[63] Razavi-Tousi SS, Szpunar JA. Effect of structural evolution of aluminum powder during ball milling on hydrogen generation in aluminum–water reaction. Int J Hydrogen Energy. 2013;38(2):795–806.

[64] Zhang DL. Processing of advanced materials using high-energy mechanical milling. Prog Mater Sci. 2004;49(3–4):537–60.

[65] Yolcular S, Karaoglu S. Activation of Al powder with NaCl-assisted milling for hydrogen generation. Energy Sources Part A: Recov Util Environ Eff. 2017;39(18):1919–27.

[66] Irankhah A, Seyed Fattahi SM, Salem M. Hydrogen generation using activated aluminum/water reaction. Int J Hydrogen Energy. 2018;43(33):15739–48.

[67] Deng Z-Y, Tang Y-B, Zhu L-L, Sakka Y, Ye J. Effect of different modification agents on hydrogen-generation by the reaction of Al with water. Int J Hydrogen Energy. 2010;35(18):9561–8.

[68] Dupiano P, Stamatis D, Dreizin EL. Hydrogen production by reacting water with mechanically milled composite aluminum-metal oxide powders. Int J Hydrogen Energy. 2011;36(8):4781–91.
[69] Fan M-q, Sun L-x, Xu F. Study of the controllable reactivity of aluminum alloys and their promising application for hydrogen generation. Energy Convers Manag. 2010;51(3):594–9.
[70] Fan M-q, XU F, Sun L. Hydrogen Generation by Hydrolysis Reaction of Ball-Milled Al-Bi Alloys. Energy Fuels. 2007;21(4):2294–8.
[71] Xiao F, Guo Y, Li J, Yang R. Hydrogen generation from hydrolysis of activated aluminum composites in tap water. Energy. 2018;157:608–14.
[72] du Preez SP, Bessarabov DG. The effects of bismuth and tin on the mechanochemical processing of aluminum-based composites for hydrogen generation purposes. Int J Hydrogen Energy. 2019;44(39):21896–21912.
[73] du Preez SP, Bessarabov DG. Hydrogen generation by means of hydrolysis using activated Al-In-Bi-Sn composites for electrochemical energy applications. Int J Electrochem Sci. 2017;12:8663–82.
[74] du Preez SP, Bessarabov DG. Hydrogen generation of mechanochemically activated Al Bi In composites. Int J Hydrogen Energy. 2017;42(26):16589–602.
[75] Wang H, Lu J, Dong SJ, Chang Y, Fu YG, Luo P. Preparation and hydrolysis of aluminum based composites for hydrogen production in pure water. Mater Trans. 2014;55(6):892–8.
[76] Wang H, Chang Y, Dong S, Lei Z, Zhu Q, Luo P, et al. Investigation on hydrogen production using multicomponent aluminum alloys at mild conditions and its mechanism. Int J Hydrogen Energy. 2013;38(3):1236–43.
[77] du Preez SP, Bessarabov DG. Hydrogen generation by the hydrolysis of mechanochemically activated aluminum-tin-indium composites in pure water. Int J Hydrogen Energy. 2018;43(46):21398–413.
[78] Fan M, Xu F, Sun L. Studies on hydrogen generation characteristics of hydrolysis of the ball milling Al-based materials in pure water. Int J Hydrogen Energy. 2007;32(14):2809–15.
[79] Wu T, Xu F, Sun L-X, Cao Z, Chu H-L, Sun Y-J, et al. Al–Li3AlH6: A novel composite with high activity for hydrogen generation. Int J Hydrogen Energy. 2014;39(20):10392–98.
[80] Liu Y, Wang X, Liu H, Dong Z, Li S, Ge H, et al. Investigation on the improved hydrolysis of aluminum–calcium hydride-salt mixture elaborated by ball milling. Energy. 2015;84:714–21.
[81] Chen C, Guan X, Wang H, Dong S, Luo P. Hydrogen generation from splitting water with Al–Bi(OH)3 composite promoted by NaCl. Int J Hydrogen Energy. 2020;45(24):13139–48.
[82] Liao L, Guo X, Xu F, Sun L, Wang T, Zhou T, et al. A high activity Al–Bi@C for hydrogen generation from Al-water reaction. Ceram Int. 2021;47(20):29064–71.
[83] Huang X-N, Lv C-J, Huang Y-X, Liu S, Wang C, Chen D. Effects of amalgam on hydrogen generation by hydrolysis of aluminum with water. Int J Hydrogen Energy. 2011;36(23):15119–24.
[84] Woodall JM, Ziebarth JT, Allen CR. The science and technology Of Al-Ga alloys as a materials for energy storage, transport and splitting water. ASME 2007 2nd Energy Nanotechnology International Conference. 2007.
[85] Ziebarth JT, Woodall JM, Kramer RA, Choi G. Liquid phase-enabled reaction of Al–Ga and Al–Ga–In–Sn alloys with water. Int J Hydrogen Energy. 2011;36(9):5271–9.
[86] Zhou Y, Dang M, Sun L, Zhai W, Dong H, Gao Q, et al. First–principle studies on the electronic structural, thermodynamics and elastic properties of Mg17Al12 intermediate phase under high pressure. Mater Res Express. 2019;6(8):0865e0861.
[87] Zhou Y, Dang M, Li X, Sun L, Dong H, Zhai W, et al. First-principles study on solid solution embrittlement effect of Ga in Al3.8Ga0.2 alloy. Mater Res Express. 2019;6(11):116541.
[88] He T, Wang W, Chen W, Chen D, Yang K. Reactivity of Al-rich alloys with water promoted by liquid Al grain boundary phases. J Mater Sci Technol. 2017;33(4):397–403.
[89] Wang W, Chen DM, Yang K. Investigation on microstructure and hydrogen generation performance of Al-rich alloys. Int J Hydrogen Energy. 2010;35(21):12011–19.
[90] Guan X, Zhou Z, Luo P, Wu F, Dong S. Effects of preparation method on the hydrolytic hydrogen production performance of Al-rich alloys. J Alloy Compd. 2019;796:210–20.
[91] He TT, Wang W, Chen W, Chen DM, Yang K. Influence of In and Sn compositions on the reactivity of Al–Ga–In–Sn alloys with water. Int J Hydrogen Energy. 2017;42(9):5627–37.
[92] Ying C, Bei L, Huihu W, Shijie D. Effects of preparation parameters and alloy elements on the hydrogen generation performance of aluminum alloy-0°C pure water reaction. Rare Met Mater Eng. 2017;46(9):2428–32.
[93] Wang F-q, Wang H-h, Wang J, Lu J, Luo P, Chang Y, et al. Effects of low melting point metals (Ga, In, Sn) on hydrolysis properties of aluminum alloys. Trans Nonferrous Met Soc China. 2016;26(1):152–9.
[94] Huang T, Gao Q, Liu D, Xu S, Guo C, Zou J, et al. Preparation of Al-Ga-In-Sn-Bi quinary alloy and its hydrogen production via water splitting. Int J Hydrogen Energy. 2015;40(5):2354–62.
[95] An Q, Hu H, Li N, Liu D, Xu S, Liu Z, et al. Effects of Bi composition on microstructure and Al-water reactivity of Al-rich alloys with low-In. Int J Hydrogen Energy. 2018;43(24):10887–95.
[96] Wei C, Liu D, Xu S, Cui T, An Q, Liu Z, et al. Effects of Cu additives on the hydrogen generation performance of Al-rich alloys. J Alloy Compd. 2018;738:105–10.
[97] Wei C, Liu Z, Wei J, Liu D, Xu S, An Q, et al. Effect of alumina on the microstructure and hydrogen production of Al-riched bulk alloys. Chem Phys Lett. 2020;738:136845.
[98] Du BD, Wang W, Chen W, Chen DM, Yang K. Grain refinement and Al-water reactivity of Al Ga In Sn alloys. Int J Hydrogen Energy. 2017;42(34):21586–96.
[99] He T, Xiong Y, Du S, Yuan Z, Liang X, Huttula M, et al. Impact of Li addition in Al-rich alloys on hydrogen production in water. J Mater Eng Perform. 2019;28(4):2459–64.
[100] Liu D, Gao Q, An Q, Wang H, Wei J, Wei C. Experimental study on Zn-doped Al-rich alloys for fast on-board hydrogen production. Crystals. 2020;10(3):167.
[101] He T, Chen W, Wang W, Ren F, Stock H-R. Effect of different Cu contents on the microstructure and hydrogen production of Al–Cu-Ga-In-Sn alloys for dissolvable materials. J Alloy Compd. 2020;821:153489.
[102] Du BD, He TT, Liu GL, Chen W, Wang YM, Wang W, et al. Al-water reactivity of Al Mg Ga In Sn alloys used for hydraulic fracturing tools. Int J Hydrogen Energy. 2018;43(15):7201–15.
[103] He T, Chen W, Wang W, Du S, Deng S. Microstructure and hydrogen production of the rapidly solidified Al–Mg-Ga-In-Sn alloy. J Alloy Compd. 2020;827:154290.
[104] An Q, Hu H, Li N, Wei J, Wei C, Wang H, et al. Strategies for improving flow rate control of hydrogen generated by Al-rich alloys for on-board applications. Int J Hydrogen Energy. 2019;44(51):27695–703.

[105] Kim Y-H, Yoo H-S, Lee J-H, Oh I-H, Park H-K, Son H-T. Study on microstructure and mechanical properties of the Al–25Cr–5Si (at%) alloy powder using gas-atomization and SPS process. Met Mater Int. 2020;27(7):2014–22.

[106] Wang C, Liu Y, Liu H, Yang T, Chen X, Yang S, et al. A novel self-assembling Al-based composite powder with high hydrogen generation efficiency. Sci Rep. 2015;5(1):17428.

[107] Beckers D, Ellendt N, Fritsching U, Uhlenwinkel V. Impact of process flow conditions on particle morphology in metal powder production via gas atomization. Adv Powder Technol. 2020;31(1):300–11.

[108] Liu Y, Liu X, Chen X, Yang S, Wang C. Hydrogen generation from hydrolysis of activated Al-Bi, Al-Sn powders prepared by gas atomization method. Int J Hydrogen Energy. 2017;42(16):10943–51.